REVISED DESIGN METHODOLOGY FOR INTEGRAL BENT CAPS IN REINFORCED CONCRETE BRIDGES

Mohamed A. Moustafa[1] and Khalid M. Mosalam[2]

[1] University of Nevada, Reno, Dept. of Civil and Environemntal Engineering, Reno, NV
[2] University of California, Berkeley, Dept. of Civil and Environemntal Engineering, Berkeley, CA
e-mail: mmoustafa@unr.edu, mosalam@berkeley.edu

ABSTRACT: The objective of this paper is to revise the design methodology of integral bent cap beams in reinforced concrete box-girder bridges. In particular, this paper provides new provisions for estimating integral bent caps effective slab width and moment capacity and study the design implications of these provisions. Currently, a conservative code-based value of 12 times the slab thickness plus beam width is used to define bent caps top and bottom flange widths to account for the box-girder slab contribution as part of the bent cap analysis and seismic capacity design. The paper presents an overview of a large-scale experimental study and full-scale bridge finite element study that investigated integral bent cap effective slab widths. A strain-based approach for estimating the effective width suggests that 18 times the slab thickness is a more accurate representation of the box-girder slab contribution to the bent cap stiffness and capacity. It is shown that using the revised effective width while considering the slab reinforcement within this effective width is more accurate than current code provisions to estimate the moment capacity of bent caps and perform capacity checks. A design case study is presented to demonstrate the implications of using the proposed revised design methodology on the seismic capacity checks for a typical California box-girder prototype bridge under different design scenarios. It is concluded that the integral bent cap revised design methodology can lead to a more economical reinforcement design in case of high seismic demands in light of AASHTO seismic design provisions.

KEYWORDS: Integral bent caps; effective width; seismic capacity checks.

1 INTRODUCTION

Highway bridges are critical infrastructure components that have been rendered seismically vulnerable during past major earthquakes, such as the 1989 Loma Prieta and the 1994 Northridge California events. It is crucial to understand the seismic response of bridge structures to improve their design and performance during seismic events. A central concept associated with the bridge seismic design practice in the United States is the capacity design approach. The core of

the capacity design approach is to direct the damage during extreme events to ductile bridge columns and maintain a capacity-protected superstructure with the goal of preventing overall collapse. Bent cap beams are superstructure components that should remain essentially elastic. Thus, accurate estimation of bent caps capacity is required as part of the capacity design procedure. The lack of accurate estimation of bent cap beam capacity can result in an uneconomical design for new construction and mislead retrofit decisions of older bridges. In cast-in-place Reinforced Concrete (RC) box-girder bridges with integral bent caps, the contribution of the box-girder slabs results in a flanged bent cap section. Proper characterization of such slab contribution, commonly referred to as the effective slab width of the flanged bent caps, can significantly affect the stiffness estimation and capacity design checks of bent caps.

Two popular seismic design guidelines for bridges in the US are the California Department of Transportation (Caltrans) Seismic Design Criteria (SDC) [1] and the American Association of State Highway and Transportation Officials (AASHTO) Guide Specifications for LRFD Seismic Bridge Design [2]. Currently, both Caltrans SDC [1] and AASHTO specifications [2] suggest an effective width of 12 times the soffit or deck slab thickness in tension or compression sides for estimating bent cap stiffness and capacity. However, slab reinforcement is not required to be considered as part of the bent cap moment capacity estimation. The goal of this study is to re-evaluate the effective slab width and integral bent caps design methodology for accurate estimation of ultimate moment capacity. The revised design methodology is simply centered on what effective slab width should be used and whether the box-girder slab reinforcement, within the effective width, should be considered as part of the capacity check.

The issue of flanged beams capacity estimation was extensively addressed in the last three decades but only for the case of building frames and flanged walls (e.g. [3-6] among others). Only few studies considered slab contributions and flanged beams effective width and effective stiffness in composite and box-girder bridges (e.g. [7,8]). However, no previous studies focused on integral bent cap ultimate moment capacity estimation and the correct effective slab width to use. To fill this knowledge gaps, the authors recently completed a comprehensive study that combined computational and experimental research to investigate the seismic response of integral bent caps [9]. This study by the authors [9] involved large-scale quasi-static and Hybrid Simulation (HS) testing of large-scale bridge subassmeblages along with detailed Finite Element (FE) modeling and analysis at the reduced-scale test specimens level. This paper presented herein extends the work recently completed and has the following objectives: (1) provide a summary of the key findings of the large-scale bridge tests in the context of revising bent caps effective width and capacity estimation; (2) determine the bent cap effective width at the full prototype bridge level for different box-girder geometries using FE models; and (3)

provide a design case study to investigate the design implications of the revised design methodology for bent cap capacity check.

The paper presents first a brief overview of the conducted experimental program (the reader is referred to [10,11] for full details). Next, sectional analysis was used to systematically define a revised design methodology to accurately estimate and reproduce the ultimate bent cap moment capacity observed from one of the tests. The experimental results were previously used to calibrate a detailed three-dimensional (3D) FE model of the test specimens [9,10]. The calibrated model parameters were utilized in this paper to develop full prototype bridge models with different box-girder geometries. The goal of this FE study is to verify whether the revised effective width found from the reduced-scale experiments is valid at the full bridge level and study the effect of the box-girder geometry on their slab contribution. Finally, a practical design case study was tackled to investigate the design implications of considering the recommended revised effective slab width along with including the slab reinforcement at the prototype bridge level.

2   EXPERIMENTAL PROGRAM
2.1 Overview
A typical California RC box-girder prototype bridge was considered to determine the geometry and configuration of the tested specimens [10], which was also used in this paper to develop the full bridge FE models and perform the design case study. A subassembly of the bent middle column and part of the cap beam along with a representative portion of the box-girder was considered as the test specimen. Two specimens with identical geometry were constructed at ¼-scale and tested in an inverted position at the Structures Laboratory at the University of California, Berkeley as shown in Fig. 1. Boundary conditions of the specimens consisted of two seat beams, cast monolithically with the specimens, at the two ends of the box-girder, and two vertical struts at the ends of the cap beam test portion. Both specimen one (SP1) and specimen two (SP2) were identical in geometry and initial design but only SP2 column was later strengthened using Carbon Fiber Reinforced Polymer (CFRP) to increase its moment capacity, and in turn, increase the demands in the bent cap into the inelastic range during testing. The design of the specimens was conducted according to Caltrans SDC [1], AASHTO LRFD Bridge Design Specifications [12], and ACI 318-08 [13]. Full details of the prototype bridge specifications and specimens geometry and design is discussed in [10].

The two specimens were both tested under combined vertical and uni- or bidirectional lateral loading as illustrated in Fig. 2. However, the lateral loading protocol varied between the two specimens where SP1 was tested under quasi-static cyclic loading and SP2 was tested using HS. HS is a mixed computational/experimental testing technique that uses an online computational

substructure subjected to earthquake loading to update the displacement input signal to a physical substructure at each time step based on the measured force feedback from the physical substructure. It is noted that a new HS system was developed and validated to test the second specimen [14]. Four sets of tests (two sets per each specimen) with different levels of constant axial load ratio (ratio of applied gravity/axial load to the column axial load capacity) were conducted (Table 1). The final loading protocols were finalized based on extensive pre-test FE analysis [9]. All tests aimed at estimating the bent cap effective slab width at different demand levels. In addition, SP2 column was strengthened and higher vertical load was used to fail the cap beam on purpose for the accurate estimation of bent cap capacity.

   The offline prescribed bidirectional cyclic loading pattern for SP1 was adopted from FEMA-461 [15] where two cycles (4 groups as shown in Fig. 2) were applied for each displacement ductility (μ) level shown in Table 1. It is noted the displacement ductility is defined as the ratio between the input displacement (u) to the displacement at first yield (u_y).

   For SP1-1 tests, an estimated value from analysis was used to define u_y and calculate the ductility ratio accordingly. For SP1-2 tests, the actual value observed for u_y from SP1-1 tests was used to define the displacement input for the desired ductility ratios for SP1-2 tests. The input for the HS tests was an online signal computed and applied based on a multi-degrees of freedom computational model using the ground motion (GM) recorded at Rinaldi station during the 1994 Northridge earthquake scaled up to 200% (Table 1). Several instrumentations were used during SP1 and SP2 tests, which included reinforcing bars strain gages, wire and linear potentiometers, load cells, and high-resolution cameras.
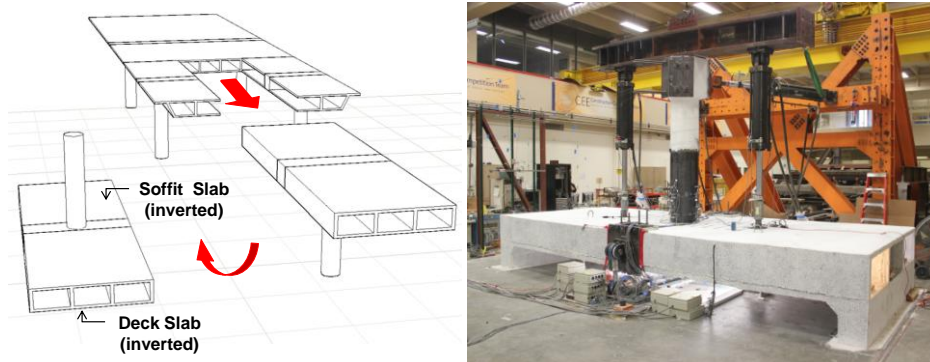

Figure 1. Inverted test specimen development and box-girder slab terminology (left); overview of the test setup and boundary conditions shown for the second specimen (SP2) HS test (right)

Table 1. Experimental program test matrix

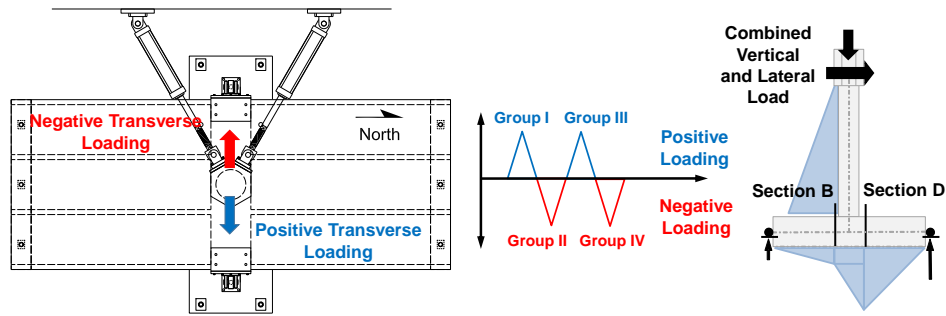| Test Set	Test Type	Axial Load Ratio	Testing scales
SP1-1	Cyclic	5%	0.25μ, 0.35μ, 0.50μ, 0.70μ, 1.0μ
SP1-2	Cyclic	10%	1.4μ, 2.0μ, 2.8μ, 4.0μ, 5.6μ, 8.0μ
SP2-1	HS	10%	25%, 50%, 75%, 100% Rinaldi GM
SP2-2	HS	15%	125%, 150%, 175%, 200% Rinaldi GM

Figure 2. Convention for loading direction (left), cyclic loading groups (middle), and bending moment distribution and critical sections in the bent cap (right)

2.2 Selected relevant results

Comprehensive assessment of the global and local behavior and seismic response of the two tested bridge subassembalegs was conducted [9-11]. Only selected results pertaining to the flexure behavior and moment capacity of the bent caps of the two tested specimens along with the summary of effective width evaluation from all tests are presented in this section.

To understand the flexure behavior of bent caps, the moment-curvature response was determined using the measured forces in the bent cap vertical supporting struts and relative displacements at the critical bent cap sections (Fig. 2). Fig. 3 shows the moment-curvature relationships for SP1 and SP2 bent caps along with the mode of failure of each test specimen. Note that the CFRP jacket was removed after SP2 test to properly investigate damage extension. SP1 experienced column plastic hinge mode of failure as required by code specifications. However, the strengthened column in SP2 did not experience extensive damage as intended because of the CFRP jacket confinement, and instead, the damage was observed in the bent cap. The figure shows about 25% difference in the bent caps moment demands, where the moment in the bent cap at section B (identified in Fig. 2) of SP1 was capped at approximately 4500 kip-in (508.4 kN-m) versus an almost 6535 kip-in (738.4 kN-m) value for SP2. This is attributed to SP1 column reaching its capacity, and in turn, limiting demands transferred to the bent cap in the cyclic test, while the bent cap experienced higher demands in SP2 due to the amplified moment transfer from the strengthened column and the higher gravity load. Moreover, the visual evidence of the bent cap concrete crushing in compression suggests that the observed

6400 kip-in (723.1 kN-m) is indeed the actual moment capacity of the bent cap. Again, bent caps are designed to be essentially elastic, but this was purposely violated for SP2 tests to obtain the moment capacity of the bent cap, and in turn, revise the design methodology of integral bent caps as presented in this paper.

   Quantifying the contribution of the box-girder slabs to the bent cap behavior, expressed in terms of the effective width (B_{eff}), was another central outcome of the experimental study. The bent cap and slab reinforcing bars in both compression and tension sides were extensively instrumented with strain gages to determine the strain distribution. A simple procedure was devised to determine the effective slab width based on the concept of an equivalent strain block [9,16]. The strain distribution was experimentally obtained and spatially extended at the two tails to determine the intercepts at zero strains. The area under the strain distribution was computed and transformed to an equivalent strain block with an effective width considering two uniform strain values, namely the minimum and mean strains of the six instrumented bars of the bent cap reinforcement at a given cross-section. An example for obtaining the equivalent strain block for 2.0μ-level SP1 test is shown in Fig. 4.
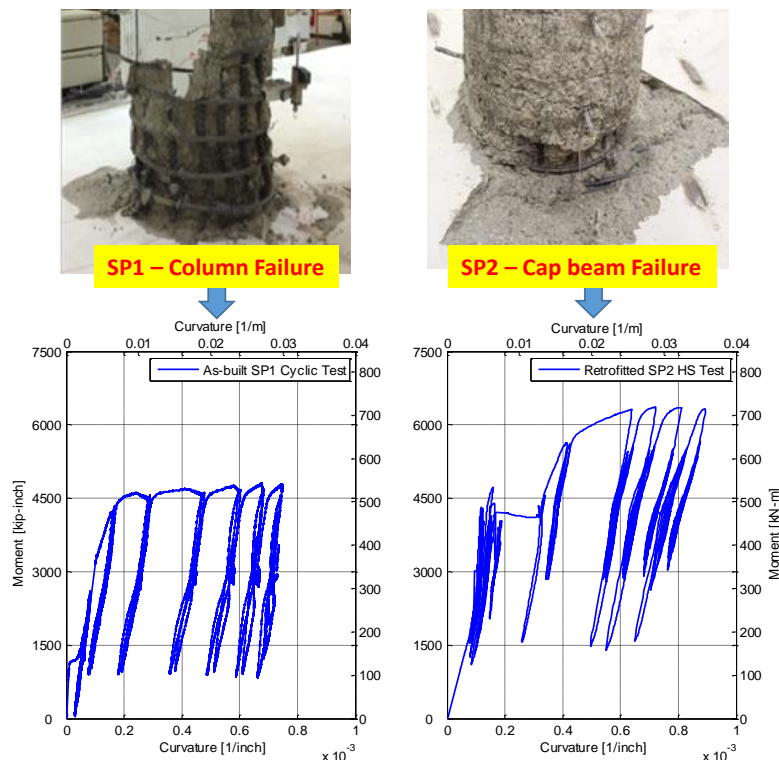

Figure 3. Comparison of the bent cap moment-curvature relationships at section B (Fig. 2) from SP1 cyclic tests and SP2 HS tests along with respective mode of failure and damage in each specimen (CFRP jacket removed for SP2)

The effective slab width was computed from all cyclic (SP1) and HS (SP2) tests, using both minimum and mean cap beam strain criteria. A summary of the mean observed effective width at section B from SP1 at the four loading groups amplitude (defined in Fig. 2) and that obtained from SP2 HS tests at peak positive and negative loading for both bent cap critical sections is shown in Figs. 5a and 5b, respectively.
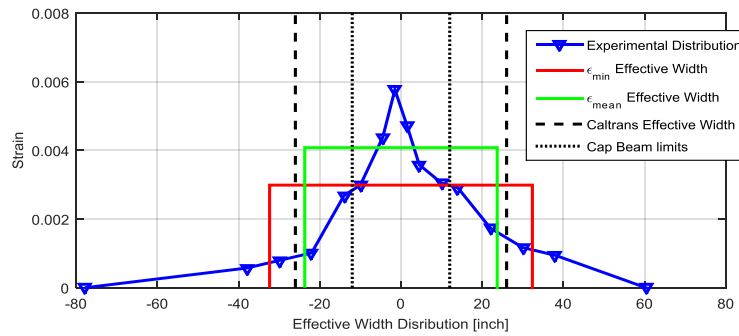

Figure 4. Sample strain block computed at section B for 2.0μ-level SP1 cyclic test
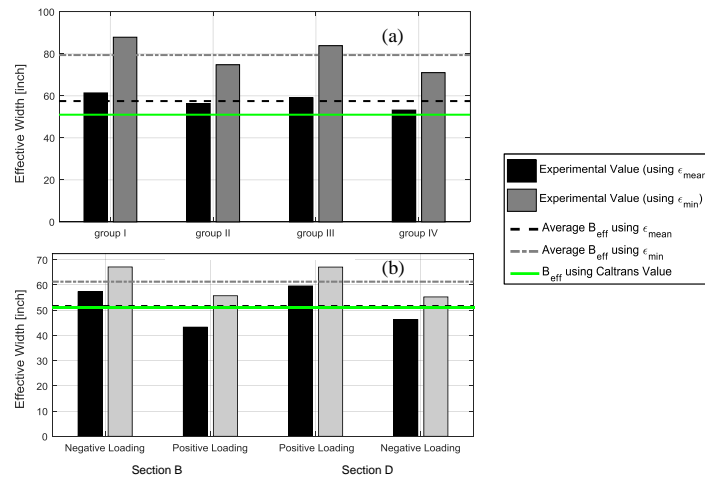

Figure 5. Mean and overall average effective width values from: (a) SP1 cyclic tests in each loading group at section D; (b) SP2 HS test runs from positive and negative loading at both sections B and D compared to Caltrans SDC effective width value [1 in. = 2.54 cm]

The figure compares the obtained effective width with the Caltrans SDC [1] and AASHTO [2] definition for the integral bent cap top and bottom effective flange width, B_{eff}, which is given as 12 times the thickness of the deck and soffit slab, respectively, plus the cap beam width. It is noted that the estimated B_{eff} from the experiments is higher than the Caltrans SDC value. When related to the slab thickness (t_s), the mean effective slab contribution from the tests ranged

from approximately $13t_s$ to $19t_s$ compared to the 12ts code value. Note that there is a difference between the overall observed effective width from SP1 and SP2, which can be attributed to the difference in the loading protocol and the axial load value that led to a different moment distribution in the bent cap. SP1 was tested under uniform cyclic loading with 5-10% axial load ratio while SP2 was tested under realistic earthquake loading using hybrid simulation and with 10-15% axial load ratio. A sectional analysis is performed next to determine the effective width and the state of the transverse slab reinforcement contribution to reproduce the experimentally determined bent cap moment capacity.

3   SECTIONAL ANALYSIS FOR TEST SPECIMEN BENT CAP

Sectional analysis is a typical step in seismic design, and particularly for capacity design checks, that aims at obtaining the moment-curvature relationship for flexure members. In bridge design, a moment-curvature analysis, or sectional analysis, is required to determine yielding and ultimate moment capacities of bent columns and cap beams in order to perform various capacity design checks. The current Caltrans [1] and AASHTO [2] provisions require calculating the integral bent cap beam capacity using the code-defined expected material properties and considering an effective slab width of 12 times the slab thickness (t_s) for box-girder slab contribution without including any slab reinforcement. These provisions for reflecting box-girder slab contributions have been challenged through this study, especially that the experimental results suggest at least $18t_s$ should be considered for slab contribution. The hypothesis is that the Caltrans and AASHTO provisions underestimate the bent cap beam capacity. To test this hypothesis, slab contributions of $12t_s$ and $18t_s$ with (w/) and without (w/o) transverse slab reinforcement were used to calculate the moment capacity of the test specimen bent cap, and then compare it against the experimentally determined value from SP2 tests. Fig. 6 shows the integral bent cap beam cross-section used in the sectional analysis in two different cases of $12t_s$ and $18t_s$ w/ slab reinforcement. It is noted that the sectional analysis should consider the expected material properties as defined by the Caltrans SDC. However, the actual determined material properties [10] were used for better comparison with the experimentally determined capacity.

The computational program XTRACT [17] was used to determine the moment-curvature relationships and absolute ultimate moment capacity of the bent cap for the different slab contribution cases. Fig. 7 shows the moment-curvature relationship obtained for three cross-section cases: $12t_s$ w/o slab reinforcement; $12t_s$ w/ slab reinforcement; and $18t_s$ w/ slab reinforcement. The figure shows that including the slab reinforcement within the defined effective slab width increases the capacity estimate significantly. Table 2 summarizes the results of different cases of slab contribution as obtained from the sectional analysis as compared to the experimentally obtained value from SP2 HS tests. It

should be noted the slab reinforcements in both compression and tension sides of the bent cap beam section were included in those cases of considering the slab reinforcement for simplicity, e.g. preserving symmetry. However, the effect of the compression steel, in general, whether from the cap beam itself or the adjacent slab reinforcement within the effective width, is minor on the capacity estimates. Thus, the notion of "slab reinforcement" in this discussion implies the tension side reinforcement even when it is not mentioned explicitly. It is concluded from the sectional analysis results that neglecting the slab reinforcement underestimates the capacity. Meanwhile, considering $18t_s$ for the effective width led to the best match with the experimentally determined upper bound for the bent cap moment capacity.
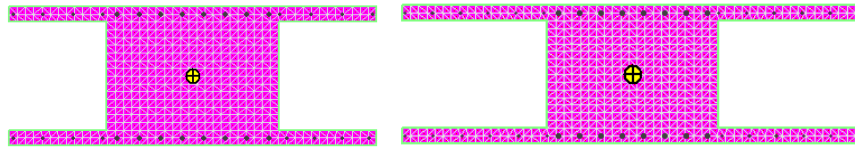

Figure 6. Two different XTRACT [17] cross-sections used for specimen bent cap sectional analysis
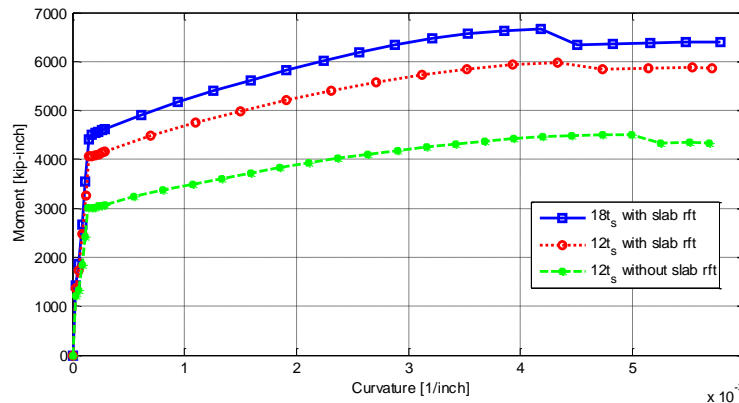

Figure 7. Moment-curvature relationships for postulated three different test specimen bent cap beam cross-sections as obtained from XTRACT sectional analysis results

Table 2. Summary of the bent cap moment capacity [kip-in] obtained from the sectional analysis

Bent cap reinforcement	$12t_s$		$18t_s$		SP2 HS Test
	w/o slab rft	w/ slab rft	w/o slab rft	w/ slab rft	
8 #5 (top & bottom)	4504	5977	4566	6855	6535

4   FE MODELING FOR FULL BRIDGE CONFIGURATIONS

The previous sections provided the discussion for accurate slab contribution and capacity estimation of integral bent caps but based on the reduced-scale tested specimen. To further extend the discussion to a full bridge level, the experiments were used to calibrate 3D FE solid models for the specimens [9,11], which was then extended in this paper to full bridge configurations. All FE modeling and analysis was done using the commercially available software DIANA [18]. The objective of this FE study is to determine the strain distribution and corresponding equivalent effective width of bent caps in full scale bridges and verify it with the experimental results from reduced-scale tests. Another objective is to check whether the effective width changes according to the box-girder geometry. The developed FE models, different considered box-girder geometric parameters, and the estimated effective slab width results for different bridge cases are presented in this section. The effect of box-girder geometry on the effective width is also discussed.

4.1 Development

A detailed sensitivity analysis and parametric study was previously conducted to calibrate the material properties and boundary conditions of 3D DIANA FE solid model for the test specimens against SP1 test results [10,11]. A sample of model verification and calibration is shown in Fig. 8 for comparing the bent cap beam moment history from SP1 tests and the FE model. The calibrated modeling parameters (e.g. concrete material behavior input parameters) were used to develop full prototype bridge models. Nine FE models were generated and adopted from the unskewed two-column bent Caltrans Academy Bridge [10] to consider different girders spacing and different soffit and deck slabs thicknesses.

A typical bridge model used solid brick elements for the concrete mesh and embedded reinforcement mesh as illustrated in Fig. 9. The total strain-based crack model that follows a smeared approach for fracture energy was used and fully calibrated for the concrete constitutive modeling of test specimens. The implementation of this model in DIANA is based on the Modified Compression Field Theory, originally proposed by Vecchio and Collins [19], and its extension to the three-dimensions proposed by Selby and Vecchio [20]. Same model parameters were used for the full bridge models. However, the bridge superstructure remained essentially elastic for all the analysis cases as required by Caltrans [1] or AASHTO [2].

All nine bridge models were analyzed under the gravity dead loads combined with lateral forces applied transversely at the two bents planes to determine the strain distribution in the bent cap and adjacent soffit and deck slabs in both compression and tension. Fig. 10a shows the strain distribution in an elevation view along the bent cap under combined gravity and lateral

loading. Fig. 10b shows the strain distribution along the cross-section at one of the critical sections in the bent cap bottom reinforcement and adjacent soffit slab transverse reinforcement. The strain results were used to estimate the equivalent effective slab width at two critical bent cap sections (Figs. 9, 10) using the same procedure previously used in the experimental program [16]. The summary of effective width results are discussed in a following section.
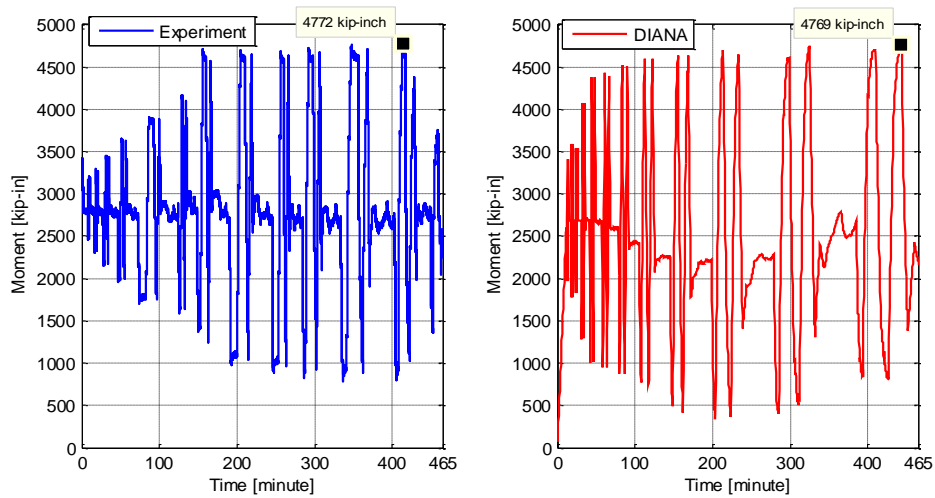

Figure 8. Bent cap beam moment history at Section B from Specimen No. 1 cyclic test and the final calibrated DIANA FE model
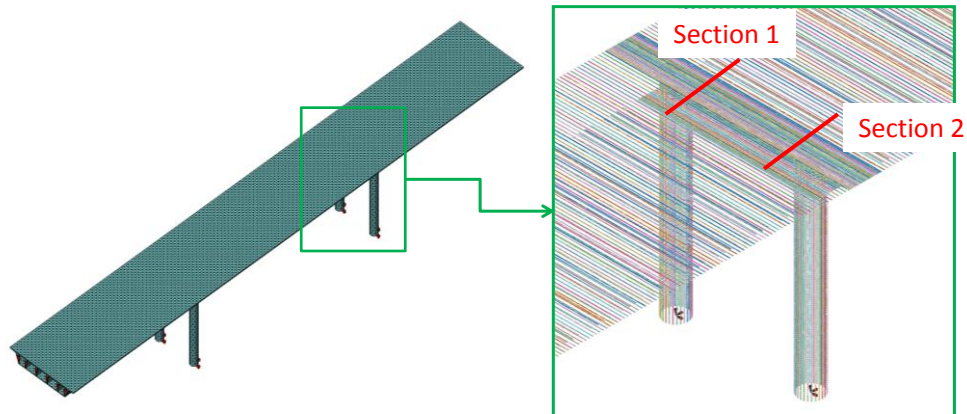

Figure 9. Typical full bridge FE model: concrete solid element mesh (left) and embedded reinforcement with identified bent cap critical bending moment sections (right)
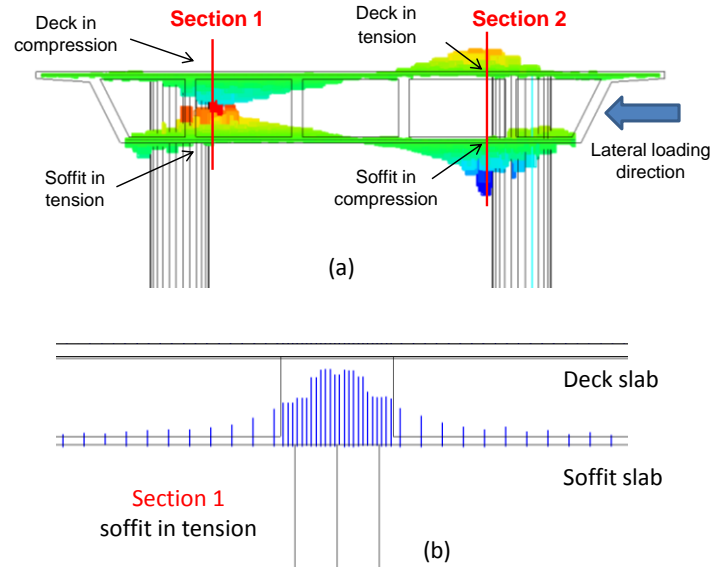
Figure 10. (a) Elevation view of the strain distribution along the bent cap and locations of maximum tensile and compression strain identified at Sections 1 and 2; (b) typical strain distribution in the bent cap bottom reinforcement and adjacent soffit slab transverse reinforcement under combined vertical and lateral loading at Section 1

4.2 Bridge geometric parameters

Several geometric parameters are associated with box-girder bridges such as the superstructure depth, the box-girders spacing, the slab thicknesses, etc. Typically, the geometric design of the bridges is governed by the traffic loads, which determine the number of lanes, and the feasible structural system, which is governed by the bents spacing and bridge spans. A bridge span will control the superstructure depth, which in turn affects the box-girder geometry. However, there is some flexibility in deciding on the girders spacing and the corresponding slab thicknesses, which are the two geometric parameters considered here. According to Caltrans [1], the box girders spacing is recommended to be within 1.5 to 2.0 times the superstructure depth (6.75 ft or 2.06 m in this case). Three values for the spacing were chosen for the first parameter to obtain a practical design and numbers of girders. These are 9-, 11-, and 14-ft clear spacing between the box-girder webs. Caltrans design aids and tables were used to choose the box-girder soffit and deck slabs thicknesses and reinforcement for each of the selected girders spacing. Thus, three sets of soffit and deck slab thicknesses were selected: 6 3/4 in. (17,1 cm), 8 1/4 in. (20.9 cm), 10 1/8 in. (25.7 cm) and 8 1/2 in. (21.6 cm), 9 1/8 in. (23.2 cm), 10 1/8 in. (25.7 cm), respectively. Accordingly, nine combinations of the chosen box-girder web spacing and slabs thicknesses were available as illustrated and summarized in Fig. 11 and Table 3. Note that each three bridge cases having similar slab

thicknesses but different web spacing are grouped together. The aspect ratio of the clear box-girder cell width-to-depth, i.e., the ratio between the clear spacing between the webs and the clear depth between the soffit and deck slabs, was calculated (Table 4) and used in results interpretation as discussed later.
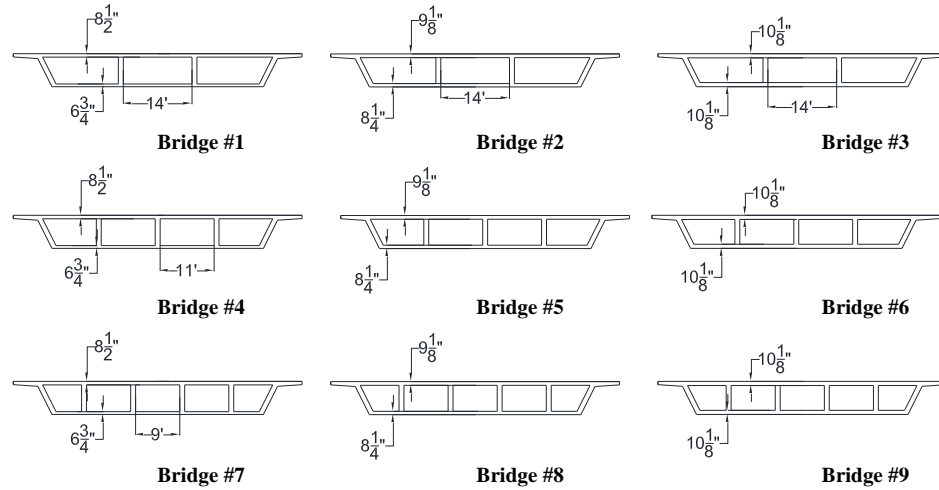

Figure 11. Cross sections of the different box-girder geometries considered in this study

Table 3. Summary of considered bridge geometries [1 in. = 2.54 cm]

Bridge Group	Group 1			Group 2			Group 3		
Bridge ID	1	4	7	2	5	8	3	6	9
Soffit slab thickness (in)	6.75	6.75	6.75	8.25	8.25	8.25	10.1	10.1	10.1
Deck slab thickness (in.)	8.50	8.50	8.50	9.13	9.13	9.13	10.1	10.1	10.1
Box-gider clear spacing, b (in)	168	132	108	168	132	108	168	132	108
Box-girder net depth, d (in)	65.7	65.7	65.7	63.6	63.6	63.6	60.7	60.7	60.7
Box-girder aspect ratio (b/d)	2.56	2.01	1.64	2.64	2.07	1.70	2.77	2.17	1.78

4.3 Strain distribution and effective width results

The strain distribution in the bent cap beam and its adjacent slabs obtained from FE results was used to find the equivalent effective slab width as before in the experimental program. Due to the relatively uniform strain distribution inside the bent cap, the mean strain value inside the bent cap was used to define the equivalent strain block. Strain values were obtained at every other reinforcement bar in the bent cap and the adjacent slabs to post-process the results and calculate the effective slab width from the equivalent strain block. A sample of the results is shown in Fig. 12 where the strain distribution and the equivalent strain block at the tension side of section 1 is presented (as an example) for all nine bridge cases. Similar to what was done before, the total effective width was calculated from the equivalent strain block and the slab

contribution and expressed in terms of the slab thickness. Figs. 13a and 13b show, respectively, the determined effective slab width and the effective slab portion expressed in terms of t_s for the bent cap at compression side at section 1 as another example for all bridges. The figure also compares the obtained values with the $12t_s$ Caltrans [1] or ASSHTO [2] code value. A summary of the calculated values for the effective slab width for the deck slab flange at sections 1 and 2 (expressed in terms of t_s) is shown in Table 4 for all bridge cases. The results mainly show that the code-based value for the effective slab width is very conservative with respect to the estimated values from the FE study. Moreover, overall average values of $17.71t_s$ and $17.56t_s$ were obtained for the equivalent deck slab flange in tension and compression, respectively. Similarly, average values of $13.28t_s$ and $12.97t_s$ were obtained for the soffit slab flange in tension and compression, respectively. These values closely agree with the experimental values estimated from both SP1 cyclic tests and SP2 HS tests, and further support the recommendation of considering $18t_s$ as a nominal revised effective slab width for integral bent caps.
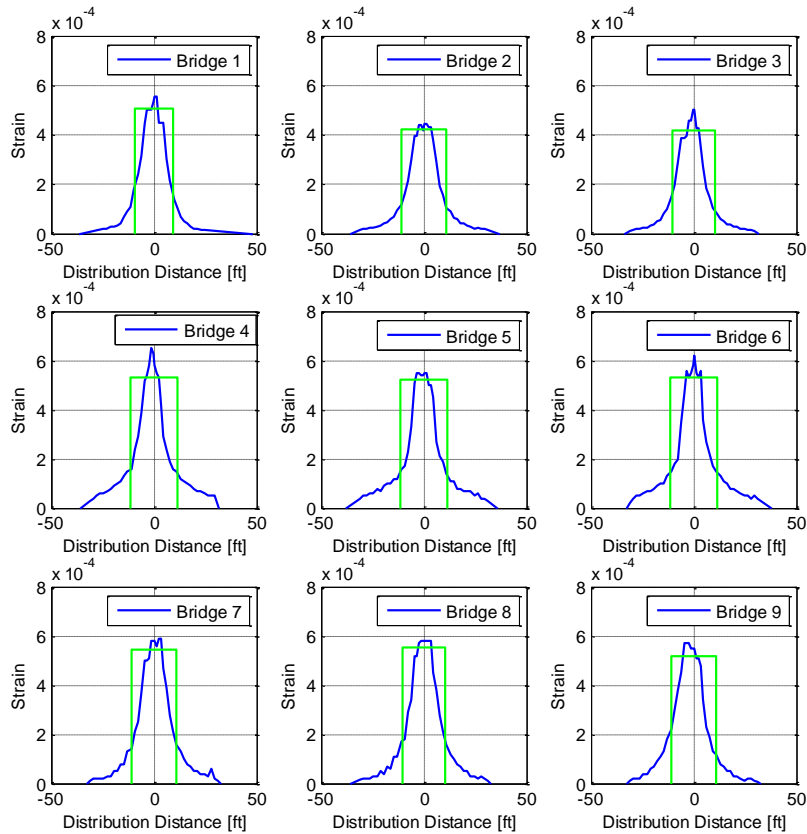

Figure 12. Summary of the strain distribution and the corresponding equivalent strain block in tension at the deck slab side at Section 1 for all bridges considered in the parametric study

Table 4. Summary of the effective slab width portion (multiples of t_s) for the bent cap deck flange n both compression (section 1) and tension (section 2) for all nine bridge cases

Bridge Group	Group 1			Group 2			Group 3			Mean
Bridge ID	1	4	7	2	5	8	3	6	9	
Section 1	18.2	22.3	18.0	17.5	20.3	17.2	14.6	16.1	15.2	17.7
Section 2	14.4	21.5	18.9	17.6	19.9	17.3	14.9	17.4	16.1	17.6
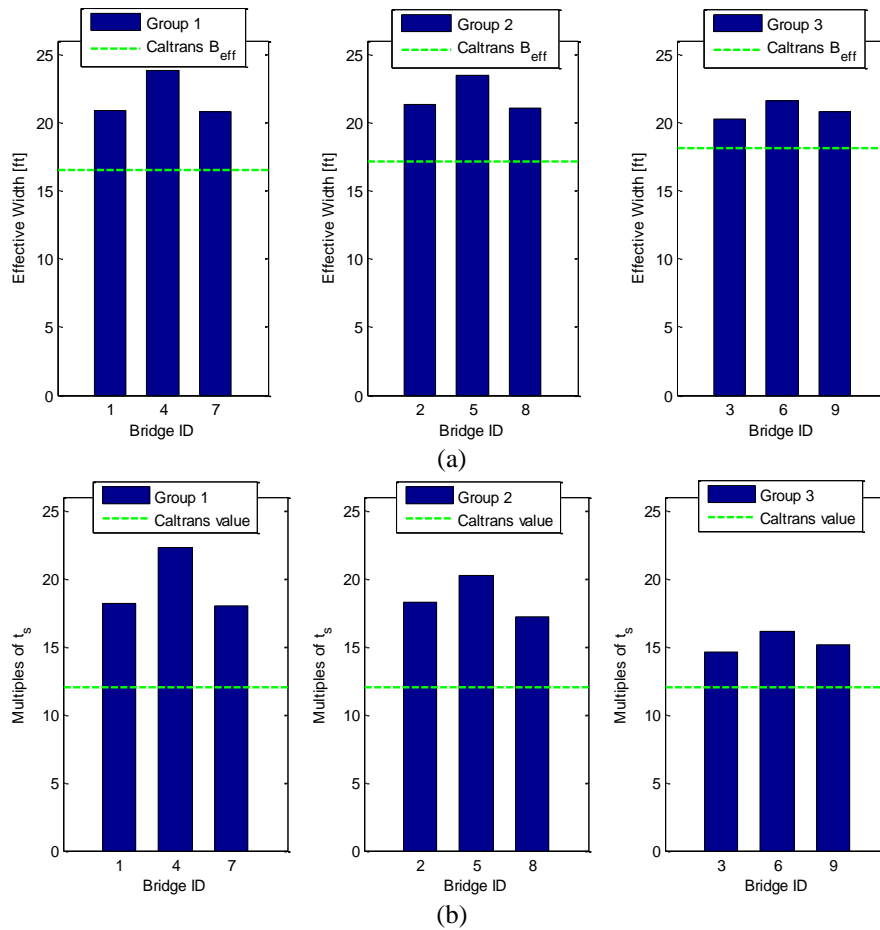
Figure 13. The effective slab portion in: (a) absolute length; (b) in terms of the slab thickness (t_s) for the bent cap deck flange in compression for all bridges along with the $12t_s$ code value

4.4 Effect of box-girder geometry

The results discussed in the previous section do not suggest a clear trend for the effect of the box-girder geometry on the effective slab width of bent caps. However, it can be seen that bridges 4, 5, and 6 where the clear box-girder web spacing is 11 ft. (3.35 m) demonstrated the largest slab contribution. To better relate the effect of both box-girder web spacing and slab thicknesses, the aspect ratio of the clear box-girder cell width-to-depth ratio is used to investigate the effective slab width variation. Ideally, it is desirable to optimize the box-girder geometry to obtain the largest slabs contribution to the bent cap beam for enhanced strength and stiffness. The different sets of slab thicknesses and web spacing are expressed as nine different values for the box-girder cell aspect ratio that varied from almost 1.6 to 2.8 (refer to Table 3 for the exact values for each of the nine bridges). Fig. 14 shows that the effective slab width is mainly influenced by the aspect ratio of box cell and the largest slab contribution, and in turn effective slab width, was observed at cell aspect ratios in the range of 2 to 2.15. Accordingly, this range for the cell aspect is recommended to take into consideration when the box-girder geometry is laid out. The figure also suggests that a larger contribution is consistently obtained from the deck slab than the soffit slab, i.e. a larger effective slab or flange width can be considered in the deck side. However, it is simpler to consider a symmetric flanged beam section when calculating the stiffness or moment capacity of integral bent caps, which also agrees with current building codes and bridge design standards [2, 12-13].
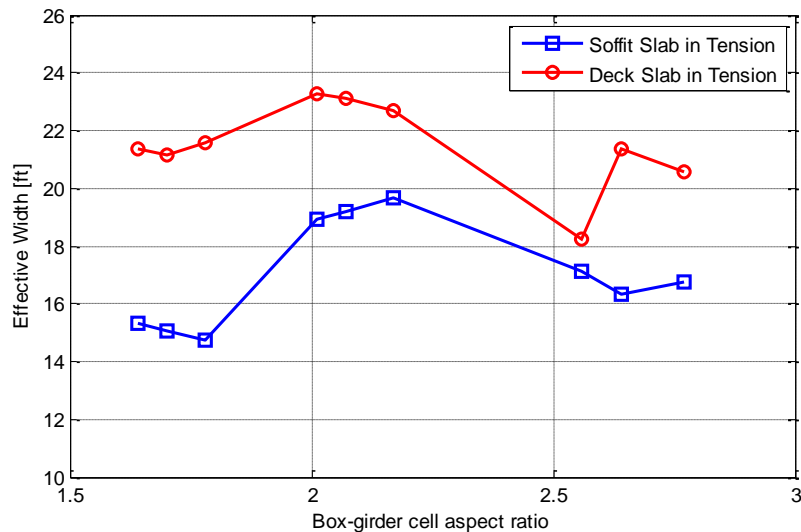

Figure 14. Variation of bent cap effective width in tension at each of the soffit flange and the deck flange with respect to the box-girder cells aspect ratio

5 DESIGN CASE STUDY

The revised design methodology presented herein for integral bent caps is centered on the new definition of the flanged beam effective width ($18t_s$) and including the slab reinforcement, within this effective width, to better estimate the bent cap strength and stiffness for seismic design and capacity checks. The effective moment of inertia of the integral bent cap, and the corresponding initial stiffness estimate for the uncracked section, should not vary significantly if a $12t_s$ or $18t_s$ effective slab width is used. On the contrary, the strength calculations and capacity estimates were found to vary significantly based on the effective slab width and the tension slab reinforcement inclusion within that effective slab width as demonstrated previously. A design case study is presented in this section based on the above drawn conclusions to identify the design implications and potential design optimization of a full-scale bridge integral bent cap. The bent cap design of the original prototype bridge (Caltrans Academy Bridge [10]) was revisited based on three different scenarios of the bent column design. For each scenario, the cap beam design, or more precisely the capacity check, was based on three cases. The first case used the provisions of the current Caltrans SDC [1] and AASHTO guide specifications for LRFD seismic design of bridges [2], i.e. using an effective slab width of $12t_s$ without including the tension slab reinforcement. The second and third cases for the full-scale bent cap design and capacity check were to include the tension slab reinforcement with $12t_s$ and $18t_s$ effective slab width, respectively. For all cases, the Caltrans SDC [1] expected material properties for a 5000 psi characteristic concrete strength and Grade 60 reinforcing steel were used to resemble actual design conditions. The relevant design criteria and the different bent column design scenarios, the bent cap capacity estimates in the three configurations described above, and performing the capacity check are presented next.
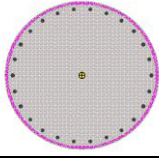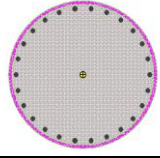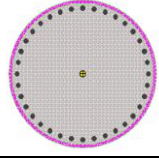
5.1 Design criteria

A typical bridge design would start with laying out the bridge spans to determine the bridge type and preliminary dimensions of different cross-sections. The next step is estimating the different loading actions primarily based on vertical gravity loads, i.e. dead loads and live traffic loads. Linear elastic analyses are then carried out to determine the different demands and finally perform LRFD design for the sections. Based on the bridge type, location, boundary and soil conditions, among other parameters, different design approaches might be undertaken to perform lateral design and checks. For the typical case considered in this study, which is a RC box-girder bridge in California, force-based and displacement-based design approaches are typically used for seismic design and checks. In particular, for the case of the integral bent cap beam that is readily dimensioned and designed using LFRD, a capacity design check is required to guarantee that the bent cap beam remains essentially

elastic during extreme seismic events. A weak column strong beam approach is used, which ties the cap beam capacity check directly to the bent column.

Three scenarios for the prototype bridge column design were considered and the bent cap design was checked accordingly. All the necessary data for design were adopted from the Caltrans design document [21] and only the relevant design information is briefly presented here for completeness. The typical practical method for designing the bent columns is to assume a longitudinal reinforcement ratio within the 1% to the 4% code limits, then perform all necessary design checks. The original prototype bridge design involved a 6-ft (1.83 m) diameter column with 1.44% reinforcement ratio, which satisfied all the design requirements and checks. To recognize possible scenarios that would require higher column reinforcement ratios, two additional designs that approximately used 2.6% and 3.5% column reinforcement ratios were used in this study. Sectional analyses were performed for all three column design scenarios and the column capacity was estimated based on the expected Caltrans material properties. A summary of the original column design and the two additional scenarios and relevant sectional analysis results are presented in Table 5.

Once the column design is completed and sectional analyses were used to compute the section capacity, the column overstrength was then estimated to use for the bent cap beam capacity check. The column overstrength is given as 1.2 times the ultimate plastic moment obtained from the sectional analysis [1,2]. To calculate the moment demands in the bent cap based on the column overstrength moment, a nonlinear planar transverse pushover analysis is typically performed. Results from 2D nonlinear model were used for the bent frame to estimate the bent cap beam moment demands [21]. The resulting positive and negative bent cap moment demands are summarized in Table 5.

Table 5. Summary of the three column scenarios for Caltrans Academy Bridge

Column Cross Section			
Diameter	6 ft	6 ft	6 ft
Longitudianl reinforcement.	26 #14	26 #18	36 #18
Reinforcement ratio	1.44%	2.56%	3.53%
Transverse reinfocement (hoops)	#8 @ 5 in.	#8 @ 5 in.	#8 @ 5 in.
Ultimate Moment M_p [kip-ft]	14,510	21,140	26,200
Overstrength Moment M_o[kip-ft]	17,410	25,370	31,440
Cap Beam M_{+ve} Demand [kip-ft]	14,970	21,820	27,040
Cap Beam M_{-ve} Demand [kip-ft]	15,670	22,830	28,300

To perform the bent cap beam capacity check, the current Caltrans and AASHTO provisions, as mentioned before, require calculating the bent cap beam capacity based on a flanged section that includes a $12t_s$ effective slab width. The readily available design for the bent cap from the vertical load LRFD design is 24#11 and 22#11 for bottom and top reinforcement, respectively, as given by the design document [21]. Additionally, the transverse slab reinforcement was required to calculate the bent cap capacity in the other two configurations adopted from the revised design methodology discussed before. To determine the box-girder slab thicknesses and transverse slab reinforcement, the design charts and tables provided by the Caltrans Memo to Designers 10-20 [22] were used. Accordingly, the design soffit and deck transverse reinforcement was #5 every 15 in. and #6 every 11 in., respectively.

5.2 Bent cap capacity

Three configurations or cross-sections were considered to investigate how the bent cap capacity can be accurately estimated and how the design can be optimized. The first configuration used the provisions of Caltrans SDC [1], or similarly the AASHTO seismic LRFD specifications [2], i.e. using an effective slab width of $12t_s$ without including the tension slab reinforcement. The second and third configurations considered the tension slab reinforcement within $12t_s$ and $18t_s$ effective slab width, respectively. It is noted that the bent cap experienced different positive and negative moment demands (Table 6). Moreover, the top (22 #11) and bottom (24 #11) bent cap reinforcement and the soffit (#5 @ 15 in.) and deck (#6 @ 11 in.) transverse slab reinforcement were not symmetric. Therefore, different capacities for positive and negative moments were calculated and considered.

The conventional sectional analysis procedure using XTRACT [17] previously adopted for determining the test specimen bent cap capacity (Section 3 of this paper) was adopted again to determine the positive and negative ultimate bent cap capacities in the three different configurations. Fig. 15 shows a typical XTRACT flanged beam section with the effective width notation defined. Fig. 15 shows the positive and negative moment-curvature relationships for the three different bent cap beam configurations.

The positive and negative moment notation is illustrated in Fig. 16. The negative moment causes sagging in the bent cap and requires top reinforcement where tension is developed. On the contrary, the positive moment causes hogging in the cap beam and requires bottom reinforcement. Accordingly, the deck (top) slab reinforcement is the tension slab reinforcement for negative moment capacity, whereas the soffit (bottom) slab reinforcement is the tension reinforcement in case of positive moment capacity.
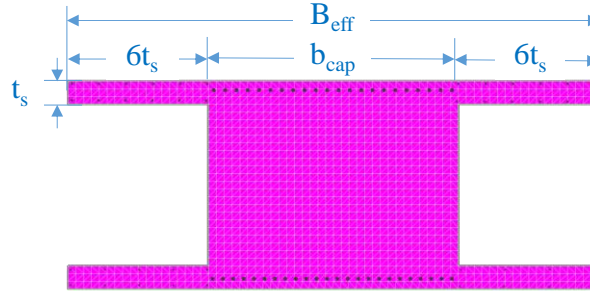
Figure 15. (a) Typical XTRACT [17] bent cap flanged cross-section for the full-scale prototype bridge when 12ts effective width is considered and slab transverse reinforcement is included;
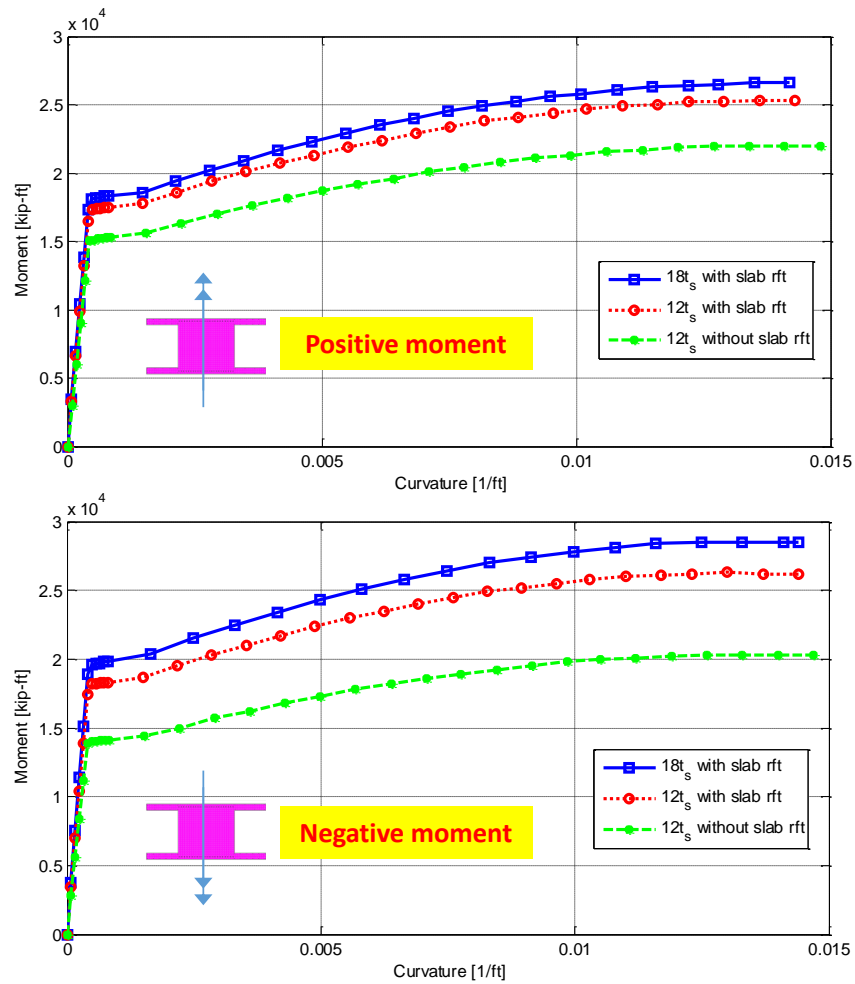

Figure 16. Moment-curvature relationships for positive and negative moment loading for the three different bent cap configurations as obtained from XTRACT [17] sectional analysis

Therefore, the positive moment capacity is slightly higher than the negative moment capacity when only the bent cap reinforcement is used in the capacity estimation (22 #11 for top versus 24 #11 for bottom), which can be observed from Fig. 16. However, the negative capacity exceeds the positive capacity when the slab reinforcement is included as observed from the same figure. The moment capacities determined from the section analyses were compared to the demands obtained from the transverse pushover analysis for the three column design scenarios to perform a capacity check as discussed next.

5.3 Seismic capacity check

The seismic capacity check is required to avoid unfavorable mode of failure. This is to guarantee that the superstructure bent cap remains essentially elastic during extreme seismic events when the ductile bent columns reach their flexural capacities. The check is performed by comparing the demand in the bent cap, which is typically estimated from a pushover analysis based on columns overstrength moments, versus the capacity that is determined using sectional analysis for a given design. In this design case study, three different scenarios for the column design were pursued and three different configurations were utilized for estimating the bent cap capacity. This resulted in a total of 18 combinations for the capacity check: nine for cases of positive demands and nine for cases of negative demands. The capacity check was performed and summarized in Tables 6 and 7 for positive and negative demand cases, respectively. Each of the two tables compares the demands in the bent cap due to the three column design scenarios versus the respective estimated capacities from three different bent cap configurations ($12t_s$ no slab rft., $12t_s$ with slab rft., and $18t_s$ with slab rft.).

It is observed from the tables that there are cases where the seismic capacity check was not satisfied and a revised bent cap beam design was required. Accordingly, the bent cap beam reinforcement was increased until the obtained bent cap capacity satisfied the capacity check. The final revised design for the cases that required additional reinforcement along with the ratio of the needed increase in the reinforcement are summarized in Tables 8 and 9 for cases of positive and negative demands, respectively. Additionally, Table 10 summarizes the overall increase in the reinforcement relative to the original design when positive and negative moment designs are combined. An assessment of the information in these tables reveals that neglecting the slab reinforcement did not require revised design only for the 1.5% column design scenario, but also required much higher reinforcement to satisfy the capacity checks for higher demands from 2.5% and 3.5% column design scenarios. Moreover, including the slab reinforcement, especially within the recommended $18t_s$ effective slab width from this study required the least design alteration and led to the most optimized bent cap beam design.

Table 6. Bent cap seismic capacity check for positive moment demands due to three design cases

Case	Column Design	Moment Demand [kip-ft]	$12t_s$ no slab rft.		$12t_s$ with slab rft.		$18t_s$ with slab rft.	
			Capacity	Satisfy Capacity Check?	Capacity	Satisfy Capacity Check?	Capacity	Satisfy Capacity Check?
1	1.44%	14,970	21,990	YES	25,260	YES	26,590	YES
2	2.58%	21,820	21,990	YES	25,260	YES	26,590	YES
3	3.50%	27,040	21,990	NO	25,260	NO	26,590	NO

Table 7. Bent cap seismic capacity check for negative moment demands due to three design cases

Case	Column Design	Moment Demand [kip-ft]	$12t_s$ no slab rft.		$12t_s$ with slab rft.		$18t_s$ with slab rft.	
			Capacity	Satisfy Capacity Check?	Capacity	Satisfy Capacity Check?	Capacity	Satisfy Capacity Check?
1	1.44%	15,670	20,270	YES	26,170	YES	28,460	YES
2	2.58%	22,830	20,270	NO	26,170	YES	28,460	YES
3	3.50%	28,300	20,270	NO	26,170	NO	28,460	YES

Table 8. Revised bent cap design and capacity check (positive moment) for three design cases

Case		1	2	3
Column design		1.44%	2.58%	3.50%
Positive moment demand [kip-ft]		14,970	21,820	27,040
$12t_s$ no slab rft.	Original Design	24 #11	24 #11	24 #11
	Original Capacity	21,990	21,990	21,990
	New Design	no change	no change	32#11
	New Capacity	no change	no change	28,790
	Increase in Rft. [%]	**0**	**0**	**33.3**
$12t_s$ with slab rft.	Original Design	24 #11	24 #11	24 #11
	Original Capacity	25,260	25,260	25,260
	New Design	no change	no change	26 #11
	New Capacity	no change	no change	27,100
	Increase in Rft. [%]	**0**	**0**	**8.3**
$18t_s$ with slab rft.	Original Design	24 #11	24 #11	24 #11
	Original Capacity	26,590	26,590	26,590
	New Design	no change	no change	26 #11
	New Capacity	no change	no change	28,680
	Increase in Rft. [%]	**0**	**0**	**8.3**

Table 9. Revised bent cap design and capacity check (negative moment) for three design cases

Case		1	2	3
Column design		1.44%	2.58%	3.50%
Negative moment demand [kip-ft]		15,670	22,830	28,300
12t_s no slab rft.	Original Design	22 #11	22 #11	22 #11
	Original Capacity	20,270	20,270	20,270
	New Design	no change	24 #11	32 #11
	New Capacity	no change	22,050	28,790
	Increase in Rft. [%]	**0**	**9.1**	**45.5**
12t_s with slab rft.	Original Design	22 #11	22 #11	22 #11
	Original Capacity	26,170	26,170	26,170
	New Design	no change	no change	26 #11
	New Capacity	no change	no change	29,740
	Increase in Rft. [%]	**0**	**0**	**8.3**
18t_s with slab rft.	Original Design	22 #11	22 #11	22 #11
	Original Capacity	28,460	28,460	28,460
	New Design	no change	no change	no change
	New Capacity	no change	no change	no change
	Increase in Rft. [%]	**0**	**0**	**0**

Table 10. Summary of additional bent cap reinforcement required to satisfy the seismic capacity check for the three different column design cases

Case		1	2	3
Column Design (long. rft. ratio) [%]		1.44	2.58	3.50
12t_s no slab rft.	Increase in Bottom rft. [%]	0.00	9.10	33.30
	Increase in Top rft. [%]	0.00	0.00	45.50
	Total Increase in rft. [%]	**0.00**	**4.55**	**39.40**
12t_s with slab rft.	Increase in Bottom rft. [%]	0.00	0.00	8.30
	Increase in Top rft. [%]	0.00	0.00	8.30
	Total Increase in rft. [%]	**0.00**	**0.00**	**8.30**
18t_s with slab rft.	Increase in Bottom rft. [%]	0.00	0.00	8.30
	Increase in Top rft. [%]	0.00	0.00	0.00
	Total Increase in rft. [%]	**0.00**	**0.00**	**4.15**

6   CONCLUSIONS

A revised design methodology for integral bent cap beams in reinforced concrete box-girder bridges was discussed and a design case study was presented in this paper. The revised methodology is centered on new provisions for estimating integral bent caps effective slab width and including the slab reinforcement in estimating bent caps stiffness and ultimate moment capacity. The paper presented the background behind the revised effective width value which included a recently completed experimental program and full prototype bridge FE study. A design case study was also presented to demonstrate the implications of using that revised design methodology on the seismic capacity

checks for a typical California box-girder prototype bridge under different design scenarios. The following conclusions can be drawn from this study:

- Experimental results from the large-scale bridge subassembalegs tests and the full-scale bridge FE study showed the $12t_s$ code value for the integral bent cap effective slab width is unnecessarily conservative. The strain distributions along the bent cap and adjacent box-girder slabs show that the box-girder effectively contribute to the bent cap response. A larger slab contribution can be obtained if the aspect ratio for the box-girder cells width-to-depth ratio is kept around 2.

- A revised value of $18t_s$ is recommended for accurate account of box-girder slab contributions, and the transverse deck and soffit slab reinforcement, within the revised effective slab width, should be included in the bent cap ultimate moment capacity and stiffness estimation.

- Based on the provided design case study for three different column design scenarios, it was shown that neglecting the slab reinforcement might not require a revised design or additional bent cap reinforcement only for lightly reinforced columns (~1.5% reinforcement ratio). However, unnecessary additional reinforcement could be needed to satisfy the current code capacity checks for columns with higher capacities (e.g. 2.5-4% reinforcement ratio or overdesigned columns retrofit). This additional reinforcement could be avoided if the proposed revised design methodology is adopted, i.e. this proposed design methodology can lead to a more economical reinforcement design in case of high seismic demand scenarios.

ACKNOWLEDGMENTS

REFERENCES

[1] Caltrans, 2013. Seismic Design Criteria 1.7. California Department of Transportation, Sacramento, CA.
[2] AASHTO, 2011. AASHTO Guide Specifications for LRFD Seismic Bridge Design, 2nd edition. American Associate of State Highway and Transportation Officials. Washington, D.C.
[3] French, C. W., & J.P. Moehle, 1991. Effect of Floor Slab on Behavior of Slab-Beam-Column Connections. ACI Special Publication, 123.
[4] Shahrooz, B.M., S.J. Pantazopoulou, & S.P. Chern, 1992. Modeling Slab Contribution in Frame Connections. Journal of Structural Engineering, 118(9), 2475-2494.
[5] Pantazopoulou, S.J., & C.W. French, 2001. Slab Participation in Practical Earthquake Design of Reinforced Concrete Frames. ACI Structural Journal, 98(4), 479-489.
[6] Hassan, M., & S. El-Tawil, 2003. Tension Flange Effective Width in Reinforced Concrete

Shear Walls. ACI Structural Journal, 100(3), 349-356.

[7] Cheung, M.S., & M.Y.T. Chan, 1978. Finite Strip Evaluation of Effective Flange Width of Bridge Girders. Canadian Journal of Civil Engineering, 5(2), 174-185.

[8] Mosalam, K.M., C.J. Naito, & S. Khaykina, 2002. Bidirectional Cyclic Performance of Reinforced Concrete Bridge Column-Superstructure Subassemblies. Earthquake Spectra, 18(4), 663-687.

[9] Moustafa, M. and K.M. Mosalam, 2015. "Seismic Response of Bent Caps in As-built and Retrofitted Reinforced Concrete Box-Girder Bridges," Engineering Structures, Vol. 98, pp. 59-73.

[10] Moustafa, M.A. and K.M. Mosalam, 2015. Structural Behavior of Column-Bent Cap Beam-Box Girder Systems in Reinforced Concrete Bridges Subjected to Gravity and Seismic Loads. Part I: Pre-test Analysis and Quasi-Static Experiments, PEER Technical Report 09/2015.

[11] Moustafa, M.A. and K.M. Mosalam, 2015. Structural Behavior of Column-Bent Cap Beam-Box Girder Systems in Reinforced Concrete Bridges Subjected to Gravity and Seismic Loads. Part II: Hybrid Simulation Tests and Post-test Analysis, PEER Technical Report 10/2015.

[12] AASHTO, 2007, LRFD Bridge Design Specification. American Associate of State Highway and Transportation Officials, Washington, D.C.

[13] ACI Committee 318, 2008. Building Code Requirements for Structural Concrete and Commentary, ACI 318-08. American Concrete Institute, Farmington Hills, MI.

[14] Moustafa, M.A. and K.M. Mosalam, 2015. Development of a Hybrid Simulation System for Multi-Degree-of-Freedom Large-Scale Testing, 6th International Conference on Advances in Experimental Structural Engineering, Urbana-Champaign, IL, USA, August 1-2, 2015.

[15] Federal Emergency Management Agency (FEMA 461), 2007. Interim Testing Protocols for Determining the Seismic Performance Characteristics of Structural and Nonstructural Components. Applied Technology Council, Redwood City, CA.

[16] Moustafa, M. A., & Mosalam, K. M., 2016. Effective Width of Integral Bent Caps in Reinforced-Concrete Box-Girder Bridges. In Geotechnical and Structural Engineering Congress 2016, pp. 77-89.

[17] Chadwell, C. B., & R.A. Imbsen, 2002. XTRACT-Cross Section Analysis Software for Structural and Earthquake Engineering. TRC, Rancho Cordova, CA, http://www.imbsen.com/xtract.htm.

[18] TNO Diana, 2014. User's Manual - Release 9.5, Delft, Netherlands.

[19] Vecchio F.J., Collins M.P., 1986. The modified compression field theory for reinforced concrete elements subjected to shear. ACI J Proc 1986; 83(2):219–31.

[20] Selby, R. G., & F.J. Vecchio, 1993. Three-dimensional Constitutive Relations for Reinforced Concrete. Technical Report 93-02, University of Toronto, Department of Civil Engineering, Toronto, Canada.

[21] Caltrans, 2006. LRFD Design Example B November 3, 2006 – Version 1.1, AASHTO, California Department of Transportation, Sacramento, CA.

[22] Caltrans, 2008. Deck and Soffit Slabs, Memo to Designers 10–20 California Department of Transportation, Sacramento, CA.